Inter*net* Electronic Journal of Molecular Design

January 2002, Volume 1, Number 1, Pages 23–36

Editor: Ovidiu Ivanciuc

Special issue dedicated to Professor Alexandru T. Balaban on the occasion of the 70th birthday
Part 1

Guest Editor: Mircea V. Diudea

De Novo Structural Prediction: Computational Design of Organometallic Complexes for the Stereoselective Binding of Prochiral Olefins

Aaron M. Gillespie and David P. White

Department of Chemistry, University of North Carolina at Wilmington, 601 South College Road, Wilmington, NC 28403

Received: November 27, 2001; Accepted: December 15, 2001; Published: January 31, 2002

Citation of the article:

A. M. Gillespie and D. P. White, De Novo Structural Prediction: Computational Design of Organometallic Complexes for the Stereoselective Binding of Prochiral Olefins, *Internet Electron. J. Mol. Des.* **2002**, *1*, 23–36, http://www.biochempress.com.

Internet Electronic Journal of Molecular Design

BioChem Press
http://www.biochempress.com

De Novo Structural Prediction: Computational Design of Organometallic Complexes for the Stereoselective Binding of Prochiral Olefins#

Aaron M. Gillespie and David P. White*

Department of Chemistry, University of North Carolina at Wilmington, 601 South College Road, Wilmington, NC 28403

Received: November 27, 2001; Accepted: December 15, 2001; Published: January 31, 2002

Internet Electron. J. Mol. Des. **2002**, *1* (1), 23–36

Abstract

Motivation. Catalytic processes involving prochiral unsaturated species frequently involve the stereoselective binding of the prochiral moiety by a chiral organometallic catalyst. The precise factors that govern the transfer of chirality from the organometallic catalyst to the substrate are largely unknown.

Method. In this study, the chiral recognition abilities of the coordinatively unsaturated $[(\eta^5\text{–}C_5R_5)Re(NO)(L)]^+$ (R = H, Me; L = PMe_3, PPh_3) fragments towards prochiral α–olefins, CH_2=CHR′ (R′ = Me, *n*–Pr, CH_2Ph (Bn), Ph, *i*–Pr, *t*–Bu, $SiMe_3$), are investigated using a combined molecular mechanics/semiempirical quantum mechanics approach. Semiempirical quantum mechanics (genetics–algorithm optimized PM3(tm) Hamiltonian) is used to obtain an accurate geometry of the $[(\eta^5\text{–}C_5R_5)Re(\eta^2\text{–prochiral olefin})(NO)(L)]^+$ complexes and molecular mechanics (ligand repulsive energy methodology with modified MMP2 force field) is used to analyze the steric interaction between prochiral α–olefin and $[(\eta^5\text{–}C_5R_5)Re(NO)(L)]^+$ fragment.

Results. A computationally derived diastereoselective excess, de_{SEQM}, is developed. Computed diastereoselective excess is compared to experiment for the $[(\eta^5\text{–}C_5H_5)Re(NO)(PPh_3)]^+$ fragment. Computed diastereoselective excesses are compared across all $[(\eta^5\text{–}C_5R_5)Re(NO)(L)]^+$ fragments order to derive ligand design criteria pertaining to the effect of the steric nature of the cyclopentadienyl and phosphine ligands on diastereoselectivity.

Conclusions. Geometries predicted by semiempirical quantum mechanical methods agree favorable with structural elements from the Cambridge database. Ligand repulsive energies are found to be sensitive measures of the steric demand of the α–olefins in the $[(\eta^5\text{–}C_5R_5)Re(NO)(L)]^+$ environments. Diastereoselective discrimination increases linearly with increasing steric demand of the $[(\eta^5\text{–}C_5R_5)Re(NO)(L)]^+$ fragments.

Keywords. Chiral recognition; PM3(tm); molecular mechanics; steric effects; ligand repulsive energy; cyclopentadienyl complexes of rhenium.

Abbreviations and notations

Cp, $(\eta^5\text{–}C_5H_5)$	the [CpRh(CO)] fragment
Cp*, $(\eta^5\text{–}C_5Me_5)$	E''_R, ligand repulsive energy computed using an SEQM–optimized geometry
de, diastereoselective excess	HOMO, highest occupied molecular orbital
de_{SEQM}, diastereoselective excess computed using SEQM	GA, genetic algorithm
DFT, density functional theory	LUMO, lowest unoccupied molecular orbital
E_R, ligand repulsive energy computed with the $Cr(CO)_5$ fragment	MM, molecular mechanics
E'_R(CpRh(CO)), ligand repulsive energy computed with	SEQM, semiempirical quantum mechanics

Dedicated on the occasion of the 70th birthday to Professor Alexandru T. Balaban.

* Correspondence author; phone: 910–962–7499; fax: 910–962–3013; E–mail: whitedp@uncwil.edu.

1 INTRODUCTION

Many important catalytic processes involve the stereorecognition of prochiral molecules. For example, asymmetric hydrogenation, used to produce the anti–Parkinson's agent L–DOPA, the anti–inflammatory Naproxen and the immunosuppressant Tacrolimus, requires the stereoselective binding of a prochiral olefin [1]. The asymmetric hydrogenation reaction has been the subject of several elegant computational studies at the molecular mechanics (MM) and *ab initio* DFT levels [2–4]. Although these studies have allowed for the understanding of the mechanism of asymmetric hydrogenation, there are few studies that address the role of steric effects in the recognition of a prochiral unsaturated species by a chiral Lewis acid [5].

Experimental work from the Gladysz laboratories has shown that the coordinatively unsaturated, 17–electron $[(\eta^5\text{–}C_5R_5)Re(NO)(PPh_3)]^+$ (R = H, Me) fragments are capable of stereoselectively binding prochiral unsaturated species [6]. Gladysz hypothesized that the steric interaction between ligands on Re and substituents on the olefin is responsible for the stereoselective binding. For simplicity consider the binding of a prochiral α–olefin, $CH_2{=}CHR'$, to chiral Lewis acids, $[(\eta^5\text{–}C_5R_5)Re(NO)(L)]^+$ (R = H, Me; L = PMe_3, PPh_3). There are four possible isomers that result when a prochiral olefin binds to the organometallic fragments, designated **I** – **IV** in Figure 1.

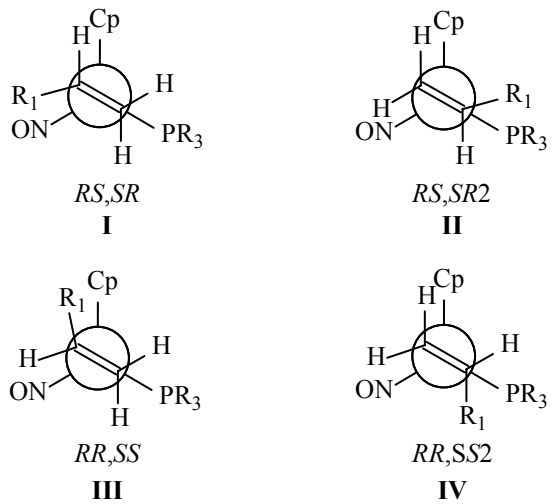

Figure 1. Four isomers that result when a prochiral α–olefin, $CH_2{=}CHR_1$, binds to a chiral Lewis acid, $[(\eta^5\text{–}C_5H_5)Re(NO)(PR_3)]^+$.

In $[(\eta^5\text{–}C_5H_5)Re(NO)(PPh_3)]^+$, the order of steric size of the ligands is PPh_3 (145°) > Cp (128°) > NO (90°) [5,7]. The isomer that contains the olefinic substituent in the interstice with the least steric congestion is **I**, the *RS*,*SR* isomer. Therefore, **I** should dominate in the binding of a prochiral olefin, which is found experimentally [6].

Brown has introduced the Ligand Repulsive Energy, E_R, as a quantitative measure of the steric demand of a ligand in a prototypical organometallic environment [8]. Ligand repulsive energy is the amount of van der Waals repulsion between a ligand and its environment. Consider $[Cr(CO)_5PR_3]$

as an example. If the Cr–P bond distance in the geometry optimized complex is r_e, $E_{vdW,R}$ is the van der Waals repulsive energy and r is a variable Cr–P distance, then

$$E_{\mathrm{R}} = -r_e\left(\frac{\partial E_{vdw,R}}{\partial r}\right) \tag{1}$$

The negative sign in equation (1) ensures that E_{R} increases as the ligand increases in steric demand. Ligand repulsive energies have been computed for a variety of different ligands in a number of prototypical environments [8–13] with different molecular mechanics force fields [14]. In general, the *trend in ligand repulsive energies is independent of both prototypical fragment and force field* [5,7–16].

Previously reported work from our laboratories has demonstrated that MM can be used to understand the steric control of prochiral olefin binding to $[(\eta^5\text{–}C_5R_5)Re(NO)(L)]^+$ (R = H, Me; L = PMe_3, PPh_3) [5]. A series of prochiral α–olefins, $CH_2{=}CHR'$, R′ = Me, *n*–Pr, CH_2Ph (Bn), Ph, *i*–Pr, *t*–Bu and $SiMe_3$, are bonded to $[(\eta^5\text{–}C_5R_5)Re(NO)(L)]^+$ to generate the isomers shown in Figure 1. Each structure was energy minimized constraining the P–Re–$C_{centroid}$–C_{ipso} torsion angle to 0 or 180°, which represents the maximal overlap between metal HOMO and olefin LUMO [6]. A combination of stochastic mechanics and low temperature molecular dynamics was used to refine the conformation of the resulting complexes [5]. Ligand repulsive energies were computed for the olefins in the $[(\eta^5\text{–}C_5R_5)Re(NO)(L)]^+$ environments.

The series of α–olefins were chosen because there are experimental data in the literature for the binding of these olefins to $[(\eta^5\text{–}C_5H_5)Re(NO)(PPh_3)]^+$ [6]. In the MM study, the *RS,SR* isomer of $[(\eta^5\text{–}C_5H_5)Re(\eta^2\text{–}CH_2{=}CHR')(NO)(PPh_3)]^+$ had both the lowest total molecular mechanics energy and the lowest ligand repulsive energy, in agreement with the literature [5]. However, attempts to derive a computational model of diastereoselectivity failed, in part because total MM energies are not good representations of the internal energy of a system and because the agreement between computed and X–ray structures could be improved with a more sophisticated computational model [5]. In this paper, we report the application of semiempirical quantum mechanics (SEQM) methods to the understanding of diastereoselective binding of prochiral olefins to chiral $[(\eta^5\text{–}C_5R_5)Re(NO)(L)]^+$ fragments.

2 COMPUTATIONAL METHODS

Molecular mechanics calculations were carried out using Cerius[2] 4.5 available from Accelrys [17] using the Universal Force Field [18] as described earlier [5]. Semiempirical calculations were carried out using Spartan 5.1 available from Wavefunction [19]. The PM3(tm) Hamiltonian was genetics algorithm (GA) optimized for prediction of geometries [20]. Conformational searches for olefin, $[(\eta^5\text{–}C_5R_5)Re(NO)(L)]^+$ fragments, and $[(\eta^5\text{–}C_5R_5)Re(\eta^2\text{–}CH_2{=}CHR')(NO)(L)]^+$ (R = H,

Me; L = PMe_3, PPh_3; R′ = Me, *n*–Pr, Bn, Ph, *i*–Pr, *t*–Bu, $SiMe_3$) were performed as reported previously [5]. Lowest energy conformers as determined by MM were directly imported without modification into Spartan 5.1. The structures were subsequently geometry optimized using the PM3(tm) level of theory [20].

3 RESULTS AND DISCUSSION

3.1 Comparison Between Computed and Predicted Structures

Structures computed with PM3(tm) compare favorably to structural elements from the CSD (Tables 1 and 2) [21].

Table 1. Comparison of Experimental and Computed Bond Distances (in Å), Angles (º), and Torsion Angles (º) for $[(\eta^5\text{–}C_5H_5)Re(\eta^2\text{–}\alpha\text{–olefin})(NO)(L)]^+$ (L = PMe_3, PPh_3) Complexes Generated Using PM3(tm)

Bond or Angle	X–Ray	Number of Data Points in CSD[21]	L = PMe_3	L = PPh_3
Re–Cp (centroid)	1.95(3)	138	1.994(6)	1.997(7)
Re–P	2.43(5)	1806	2.44(6)	2.47(1)
Re–N	1.76(4)	207	1.80(2)	1.81(2)
Re–CH_2 (olefin)	2.24(7)	56	2.08(1)	2.08(1)
Re–C_{ipso} (olefin)	2.26(10)	56	2.10(2)	2.10(2)
Re–Centroid (olefin)	2.13(8)	56	1.95(1)	1.95(1)
N–O	1.19(3)	207	1.22(3)	1.204(2)
C=C	1.41(4)	56	1.502(6)	1.499(3)
Re–N–O	174(3)	207	171(3)	169(3)
Cp(centroid)–Re–P	120(3)	57	117(1)	117(1)
Re–C(olefin centroid)–C_{ipso}	91(1)	9	90.9(8)	90.8(9)
Re–C(olefin centroid)–C_{ipso}–P	–2(16)	9	–172(2), 10(2)	–175(2), 9(5)

Table 2. Comparison of Experimental and Computed Bond Distances (in Å), Angles (º), and Torsion Angles (º) for $[(\eta^5\text{–}C_5Me_5)Re(\eta^2\text{–}\alpha\text{–olefin})(NO)(L)]^+$ (L = PMe_3; PPh_3) Complexes Generated Using SEQM (PM3(tm))

Bond or Angle	X–Ray	Number of Data Points in CSD[21]	L = PMe_3	L = PPh_3
Re–Cp* (centroid)	1.97(2)	146	2.03(4)	2.04(1)
Re–P	2.43(5)	1806	2.45(1)	2.475(9)
Re–N	1.76(4)	207	1.79(2)	1.79(2)
Re–CH_2 (olefin)	2.24(7)	56	2.080(7)	2.079(8)
Re–C_{ipso} (olefin)	2.26(10)	56	2.11(2)	2.11(1)
Re–Centroid (olefin)	2.13(8)	56	1.954(9)	1.957(7)
N–O	1.19(3)	207	1.207(2)	1.207(3)
C=C	1.41(4)	56	1.501(7)	1.498(3)
Re–N–O	174(3)	207	173(2)	173(2)
Cp*(centroid)–Re–P	126(4)	41	120.2(7)	120(1)
Re–C(olefin centroid)–C_{ipso}	91(1)	9	91.0(8)	91.3(7)
Re–C(olefin centroid)–C_{ipso}–P	–2(16)	9	–166(5), 11(4)	–171(6), 11(8)

Agreement between computed and experimental structures follow the same trends for both Cp and Cp* complexes. For example, PM3(tm) overstates both the Re–Cp(centroid) and Re–Cp*(centroid) distances, although the computed distances are within three standard deviations of the X–ray structures. Similarly, PM3(tm) understates the Re–olefin distances. Problems with modeling the π–effects of the ligands are also reflected in the N–O and C=C bond distances, which

are overstated in the PM3(tm) structures. The elongation of computed N–O and C=C bonds implies that PM3(tm) places too much electron density on the metal, which overestimates the amount of π–backbonding in the complexes.

Literature reports that the olefin coordinates to the metal to maximize the overlap between metal HOMO and olefinic LUMO [6,22–24]. Gladysz has noted that this electronic arrangement overrides the steric preference for the olefin to adopt different orientations. Therefore, the Re–C(olefin)–C_{ipso}–P torsion angle should be either 0° or 180°. Tables 1 and 2 indicate that the PM3(tm) calculations reliably reproduce these torsion angles, which is impossible with MM calculations [5].

For electronic reasons, the Re–olefin bond vector should be normal to the plane of the olefin, which is reflected in the Re–C(olefin centroid)–C_{ipso} angle, which is reproduced in the PM3(tm) structures (Tables 1 and 2). Molecular mechanics optimized structures with the Universal Force Field have an average Re–C(olefin centroid)–C_{ipso} angle of 101(5)°, indicating that there is an unfavorable steric interaction between olefinic substituent and metal fragment that forces the deviation from normality [5]. The difference between the two Re–C(olefin) distances is 0.28 Å with MM/UFF [5], but only 0.02 Å with SEQM/PM3(tm).

The Cp(centroid)–Re–P angle is a good indication of the difference in steric demand of the Cp versus Cp* structures. X–Ray structures show that the cyclopentadienyl(centroid)–Re–P angle is 120(3)º for the Cp ligand and 126(4)º for the Cp* ligand. SEQM understates both these angles (117(1)º for the Cp ligand and 120(1)º for the Cp* ligand), which implies that SEQM can understate the steric bulk of the Cp* ligand.

In summary, PM3(tm) provides better structures than MM for the $[(\eta^5\text{–}C_5R_5)Re(\eta^2\text{–olefin})(NO)(L)]^+$ complexes, which is in agreement with previously reported results for the PM3(tm) method [20].

3.2 Steric Sizes of Olefins from SEQM-Optimized Structures

To our knowledge, there are no reports of ligand repulsive energy calculations on structures optimized using PM3(tm). The ligand repulsive energy computed from an SEQM–optimized geometry is called E''_R. (The label E_R is reserved for ligand repulsive energies computed in the $Cr(CO)_5$ environment.) Ligand repulsive energies are computed as follows: the PM3(tm)–optimized structure is exported from Spartan as a pdb file and converted into a Cerius[2] bgf file. The bgf file is submitted to ERCODE, which was produced in our laboratories to compute ligand repulsive energies [14]. ERCODE uses the van der Waals parameters from either the Universal Force Field [18,25] or the MMP2 force field [26,27]. Tables 3 and 4 list the ligand repulsive energies and PM3(tm) enthalpies of formation for the complexes studied.

In general, the ligand repulsive energies show the expected increase as the steric bulk of the olefin increases. Consider the *RS*,*SR* isomers (Figure 1): if the benzyl datum is excluded [5], then

there is an excellent linear relationship between ligand repulsive energies computed for the α–olefins in the $[(\eta^5–C_5R_5)Re(NO)(L)]^+$ (R = H, Me; L = PMe_3, PPh_3) environments and Brown's ligand repulsive energies, E_R computed in the $Cr(CO)_5$ environment (Figure 2) [12]. Previously, we noted that the ligand repulsive energies for the *RS,SR* isomers correlate better with E_R (computed in the $Cr(CO)_5$ environment) than the other three olefin isomers illustrated in Figure 1 (r = 0.566 – 0.944 for plots of E''_R versus E_R for the *RS,SR*2, *RR,SS*, and *RR,SS* isomers) [5].

Table 3. Comparison of Ligand Repulsive Energies, E''_R in kcal/mol, and PM3(tm) Heats of Formation, ΔH in kcal/mol, Boltzmann Weights, w_i, and Boltzmann Averaged E''_R Values for η^2–Olefins, CH_2=CHR, in the $[(\eta^5–C_5H_5)Re(NO)(L)]^+$ (L = PMe_3, PPh_3) Environments

R	Isomer[a]	L = PMe_3				L = PPh_3			
		ΔH	E''_R	w_i[b]	$<E''_R>$[c]	ΔH	E''_R	w_i[b]	$<E''_R>$[c]
Me	RS,SR	–231.4	31.0	0.7916	0.7916	–110.4	42.4	0.7387	0.7387
	*RS,SR*2	–229.9	36.0	0.0683	2×10^{-5}	–108.1	55.9	0.0171	2×10^{-12}
	RR,SS	–230.3	44.1	0.1327	3×10^{-11}	–109.7	50.2	0.2441	5×10^{-7}
	*RR,SS*2	–228.6	34.2	0.0074	3×10^{-5}	–105.4	55.9	0.0002	2×10^{-14}
n–Pr	RS,SR	–241.6	31.1	0.8284	0.8284	–120.5	42.6	0.9997	0.9997
	*RS,SR*2	–239.9	36.8	0.0513	4×10^{-6}	–113.9	68.4	0.0000	2×10^{-24}
	RR,SS	–240.4	42.8	0.1150	3×10^{-10}	–115.1	64.5	0.0001	9×10^{-21}
	*RR,SS*2	–238.6	36.0	0.0054	2×10^{-6}	–115.4	60.8	0.0002	1×10^{-17}
Bn	RS,SR	–202.7	30.5	0.8437	0.8437	–81.6	42.0	0.7782	0.7782
	*RS,SR*2	–200.9	37.2	0.0361	5×10^{-7}	–78.7	62.1	0.0059	1×10^{-17}
	RR,SS	–201.6	39.7	0.1149	2×10^{-8}	–80.9	51.7	0.2158	2×10^{-8}
	*RR,SS*2	–199.7	36.5	0.0053	2×10^{-7}	–76.6	61.7	0.0002	7×10^{-19}
Ph	RS,SR	–197.0	37.4	0.9103	0.9103	–75.8	49.6	0.8790	0.8790
	*RS,SR*2	–194.1	65.1	0.0071	4×10^{-23}	–70.8	91.9	0.0002	2×10^{-35}
	RR,SS	–195.6	79.5	0.0798	1×10^{-32}	–74.6	81.6	0.1208	4×10^{-25}
	*RR,SS*2	–193.5	65.2	0.0028	1×10^{-23}	–67.6	57.5	0.0000	1×10^{-12}
i–Pr	RS,SR	–236.2	43.6	0.0208	0.0208	–114.4	59.6	0.0255	0.0255
	*RS,SR*2	–235.7	59.5	0.0092	2×10^{-14}	–114.0	68.5	0.0128	4×10^{-9}
	RR,SS	–238.5	48.3	0.9694	0.0004	–116.6	61.5	0.9616	0.0420
	*RR,SS*2	–234.1	49.9	0.0006	1×10^{-8}	–110.9	71.2	0.0001	2×10^{-13}
t–Bu	RS,SR	–241.3	44.5	0.9232	0.9232	–120.1	56.7	0.8275	0.8275
	*RS,SR*2	–239.4	68.1	0.0378	2×10^{-19}	–113.6	100.4	0.0000	1×10^{-37}
	RR,SS	–239.4	65.1	0.0390	3×10^{-17}	–119.2	72.8	0.1725	3×10^{-13}
	*RR,SS*2	–235.4	54.3	0.0000	3×10^{-12}	–111.2	98.1	0.0000	1×10^{-37}
$SiMe_3$	RS,SR	–275.3	35.5	0.0085	0.0085	–153.5	47.2	0.1767	0.1767
	*RS,SR*2	–278.1	49.4	0.9845	6×10^{-17}	–153.7	85.6	0.2750	2×10^{-29}
	RR,SS	–275.1	63.9	0.0065	9×10^{-24}	–154.2	74.9	0.5484	3×10^{-21}
	*RR,SS*2	–273.5	50.6	0.0005	3×10^{-15}	–147.3	79.0	0.0000	3×10^{-29}

[a] The stereochemistry of the isomer is illustrated in Figure 1.
[b] See equation (3).
[c] See equation (4).

Better correlations are observed when the ligand repulsive energies for the *RS,SR* SEQM–optimized isomers are plotted against E'_R(CpRh(CO)) instead of $E_R(Cr(CO)_5)$ (Figure 3). The geometric similarity between [CpRh(CO)] and $[(\eta^5–C_5R_5)Re(NO)(L)]^+$ fragments is the most likely cause of the improved correlations. The other three isomers illustrated in Figure 1 correlate as poorly with E'_R(CpRh(CO)) as with $E_R(Cr(CO)_5)$ (r between 0.562 and 0.927).

Table 4. Comparison of Ligand Repulsive Energies, E''_R in kcal/mol, and PM3(tm) Heats of Formation, ΔH in kcal/mol, Boltzmann Weights, w_i, and Boltzmann Averaged E''_R Values for η^2–Olefins, CH_2=CHR, in the $[(\eta^5–C_5Me_5)Re(NO)(L)]^+$ (L = PMe_3, PPh_3) Environments

R	Isomer[a]	L = PMe_3				L = PPh_3			
		ΔH	E''_R	w_i[b]	$<E''_R>$[c]	ΔH	E''_R	w_i[b]	$<E''_R>$[c]
Me	RS,SR	–265.3	39.2	0.9672	0.9672	–141.4	54.4	0.9967	0.9967
	*RS,SR*2	–263.2	44.1	0.0293	8×10^{-6}	–137.9	68.4	0.0031	2×10^{-13}
	RR,SS	–260.8	55.3	0.0005	8×10^{-16}	–136.1	64.7	0.0001	4×10^{-12}
	*RR,SS*2	–261.9	44.4	0.0030	5×10^{-7}	–135.0	68.9	0.0000	6×10^{-16}
n–Pr	RS,SR	–275.5	39.6	0.9730	0.9273	–151.5	54.5	0.9969	0.9969
	*RS,SR*2	–273.3	45.8	0.0246	7×10^{-7}	–148.1	73.5	0.0029	3×10^{-17}
	RR,SS	–270.7	57.0	0.0003	5×10^{-17}	–146.2	63.7	0.0001	2×10^{-11}
	*RR,SS*2	–271.9	47.2	0.0022	6×10^{-9}	–144.9	75.0	0.0000	1×10^{-20}
Bn	RS,SR	–236.8	42.2	0.9782	0.9782	–112.9	58.3	0.9987	0.9987
	*RS,SR*2	–234.5	49.4	0.0197	1×10^{-7}	–108.7	73.1	0.0008	1×10^{-14}
	RR,SS	–231.9	56.2	0.0002	1×10^{-14}	–108.3	66.6	0.0004	3×10^{-10}
	*RR,SS*2	–233.1	49.5	0.0019	8×10^{-9}	–106.2	79.4	0.0000	4×10^{-21}
Ph	RS,SR	–229.6	51.1	0.9452	0.9453	–105.1	67.0	0.9980	0.9980
	*RS,SR*2	–227.8	78.8	0.0421	2×10^{-22}	–100.0	127	0.0002	4×10^{-48}
	RR,SS	–224.7	97.8	0.0002	2×10^{-38}	–101.3	112	0.0018	2×10^{-36}
	*RR,SS*2	–227.0	78.9	0.0125	5×10^{-23}	–98.5	99.6	0.0000	2×10^{-29}
i–Pr	RS,SR	–271.8	44.9	0.9340	0.9340	–149.1	62.8	1.0000	1.000
	*RS,SR*2	–270.3	65.9	0.0653	3×10^{-17}	–141.2	85.3	0.0000	5×10^{-23}
	RR,SS	–267.3	64.1	0.0004	4×10^{-18}	–142.1	72.2	0.0000	1×10^{-12}
	*RR,SS*2	–266.9	61.4	0.0002	2×10^{-16}	–140.1	83.2	0.0000	3×10^{-22}
t–Bu	RS,SR	–274.2	54.5	0.9976	0.9977	–149.7	70.8	1.0000	1.000
	*RS,SR*2	–270.6	84.2	0.0023	4×10^{-25}	–141.1	107	0.0000	2×10^{-33}
	RR,SS	–262.8	73.9	0.0000	3×10^{-23}	–141.9	92.9	0.0000	1×10^{-22}
	*RR,SS*2	–267.5	69.5	0.0000	1×10^{-16}	–140.1	118	0.0000	1×10^{-42}
$SiMe_3$	RS,SR	–308.9	46.4	0.1452	0.1452	–184.2	62.7	1.0000	1.000
	*RS,SR*2	–309.5	66.4	0.4254	9×10^{-16}	–177.6	101	0.0000	2×10^{-33}
	RR,SS	–309.5	70.4	0.4269	1×10^{-18}	–176.7	85.1	0.0000	1×10^{-22}
	*RR,SS*2	–306.5	68.8	0.0025	9×10^{-20}	–175.5	94.3	0.0000	3×10^{-30}

[a] The stereochemistry of the isomer is illustrated in Figure 1.
[b] See equation (3).
[c] See equation (4).

In the plots of E''_R versus $E_R(Cr(CO)_5)$ (Figure 2) the slopes increase as follows $[CpRe(NO)(PMe_3)]^+$ (0.540) < $[CpRe(NO)(PPh_3)]^+$ (0.592) < $[Cp^*Re(NO)(PMe_3)]^+$ (0.598) < $[Cp^*Re(NO)(PPh_3)]^+$ (0.650). In the plot of E''_R versus $E'_R(CpRh(CO))$ (Figure 3) the slopes increase $[CpRe(NO)(PMe_3)]^+$ (0.829) < $[Cp^*Re(NO)(PMe_3)]^+$ (0.868) < $[CpRe(NO)(PPh_3)]^+$ (0.942) < $[Cp^*Re(NO)(PPh_3)]^+$ (0.962). Brown and White have shown that when the ligand repulsive energies for one set of ligands computed with one fragment are plotted against the ligand repulsive energies for the same ligands computed with a different fragment, then the steric demand of the two fragments can be compared [5,10–14]. In Figure 2, the slopes of the regression lines all are less than unity, which means that the organorhenium fragment is, on average, less sterically congested than the $Cr(CO)_5$ fragment from the perspective of the η^2–bound α–olefins. However, the slopes of the regression lines in Figure 3 are all above 0.8, which implies that the relative steric demand of the [CpRh(CO)] and $[(\eta^5–C_5R_5)Re(NO)(L)]^+$ fragments are similar on average, as

computed from the perspective of η^2–bonded olefins.

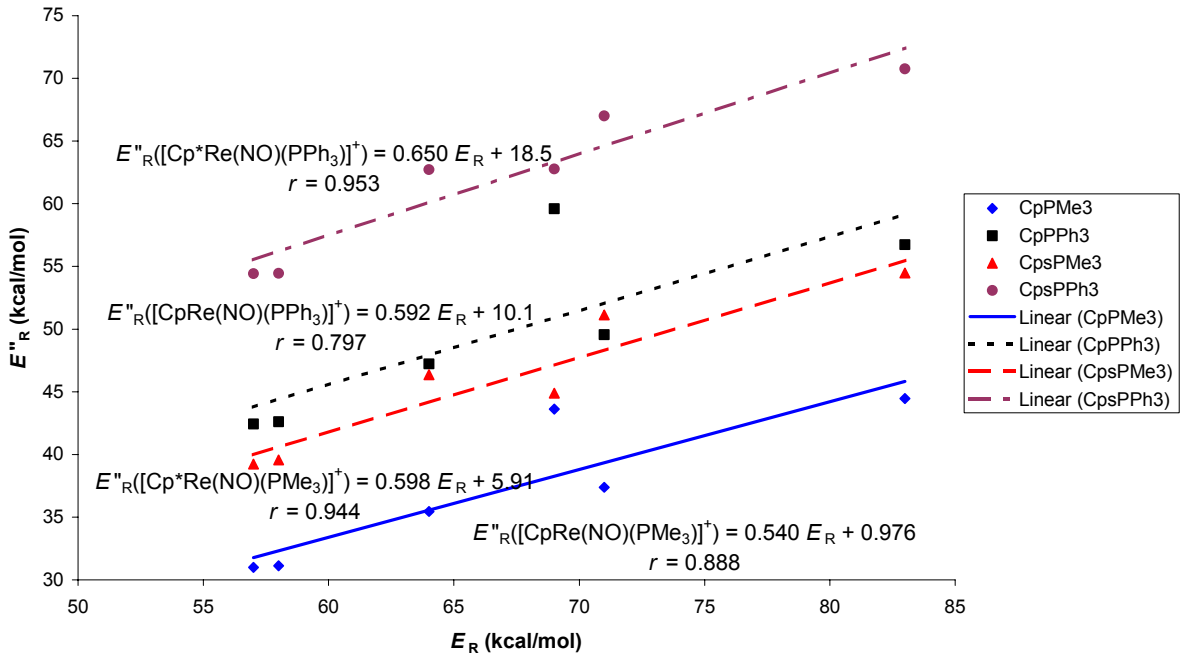

Figure 2. Plot of ligand repulsive energy computed for the *RS*,*SR* isomers of the olefins with the $[(\eta^5\text{–}C_5R_5)Re(NO)(L)]^+$ fragments (R = H, Me; L = PMe_3; PPh_3) versus Brown's E_R values computed with the $Cr(CO)_5$ fragment [12].

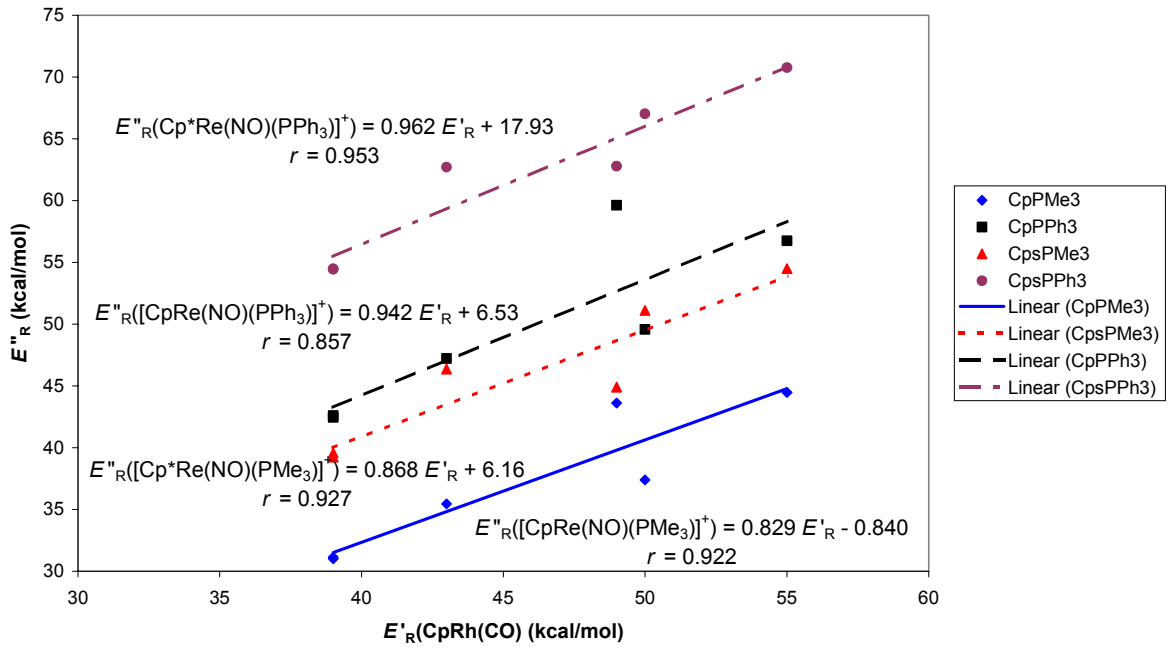

Figure 3. Plot of ligand repulsive energy computed for the *RS*,*SR* olefin isomers with the $[(\eta^5\text{–}C_5R_5)Re(NO)(L)]^+$ fragments (R = H, Me; L = PMe_3; PPh_3) versus Brown's E'_R values computed with the [CpRh(CO)] fragment [12].

As the prototypical fragment bonded to the α–olefins gets larger from $Cr(CO)_5$ to [CpRh(CO)], the steric demand of the $[CpRe(NO)(PPh_3)]^+$ and $[Cp^*Re(NO)(PMe_3)]^+$ fragments experienced by

the η^2–bonded olefins swap. When ligand repulsive energies for the $[CpRe(NO)(PMe_3)]^+$ and $[Cp^*Re(NO)(PMe_3)]^+$ fragments are plotted against each other, the slope is 1.04 (r = 0.967), which implies that from the average perspective of all the η^2–olefins, the $[Cp^*Re(NO)(PMe_3)]^+$ fragment is larger than $[CpRe(NO)(PMe_3)]^+$, as expected. Similarly, when E''_R computed with the $[CpRe(NO)(PPh_3)]^+$ is plotted against E''_R computed with the $[Cp^*Re(NO)(PPh_3)]^+$ fragment, the slope of the line is 1.09 (Figure 4), which implies the $[Cp^*Re(NO)(PPh_3)]^+$ fragment is more sterically demanding than the $[CpRe(NO)(PPh_3)]^+$ fragment, also as expected.

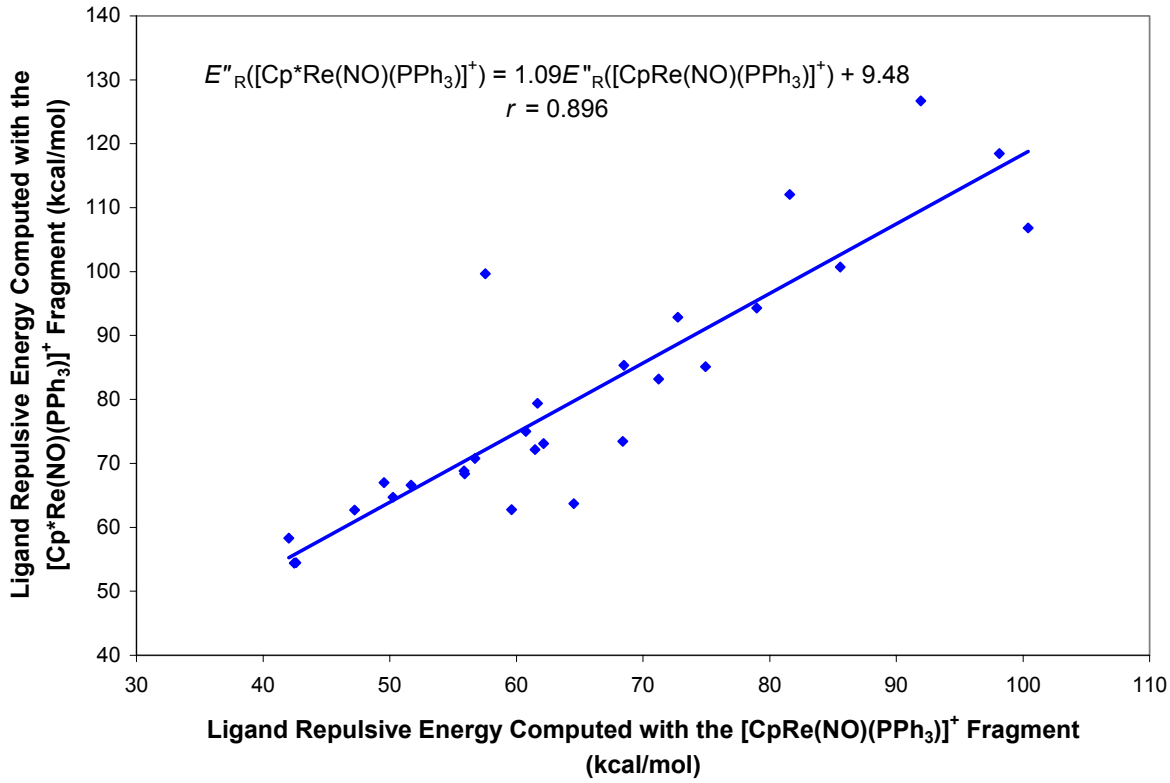

Figure 4. Plot of ligand repulsive energy computed for the olefins listed in Table 3 computed with the $[Cp^*Re(NO)(PPh_3)]^+$ fragment versus the ligand repulsive energies computed with the $[CpRe(NO)(PPh_3)]^+$ fragment.

To determine which of the $[CpRe(NO)(PPh_3)]^+$ and $[Cp^*Re(NO)(PMe_3)]^+$ fragments is larger from the perspective of our set of α–olefins, the ligand repulsive energies computed in these two environments are plotted against each other (Figure 5). The correlation coefficient for the plot, r = 0.758, is lower than those for the other correlations (Figures 2 – 4) since some olefins experience greater steric repulsion from the $[Cp^*Re(NO)(PMe_3)]^+$ fragment, while others experience greater steric repulsion from the $[CpRe(NO)(PPh_3)]^+$ fragment. However, *on average the* $[Cp^*Re(NO)(PMe_3)]^+$ *fragment is more sterically demanding than the* $[CpRe(NO)(PPh_3)]^+$ *fragment across the full range of α-olefins studied.*

In summary, ligand repulsive energy data indicate that the steric demand of the fragments increase: $[CpRe(NO)(PMe_3)]^+ < [CpRe(NO)(PPh_3)]^+ < [Cp^*Re(NO)(PMe_3)]^+ < [Cp^*Re(NO)(PPh_3)]^+$. If we

sum the cone angles [7,16,28,29] of the ligands attached to the metal in each of the above fragments, assuming that the cone angle of the linear NO ligand is approximately the same as that for CO [5], then we find the total fragment cone angles follow the same trend as ligand repulsive energies: $[CpRe(NO)(PMe_3)]^+$ (246º) < $[CpRe(NO)(PPh_3)]^+$ (273º) < $[Cp^*Re(NO)(PMe_3)]^+$ (300º) < $[Cp^*Re(NO)(PPh_3)]^+$ (327º). Ligand repulsive energies provide a quantitative measure of the steric demand of an η^2–bonded olefin in the $[(\eta^5\text{–}C_5R_5)Re(NO(L)]^+$, R = H or Me, L = PMe_3 or PPh_3, environments geometry optimized using PM3(tm).

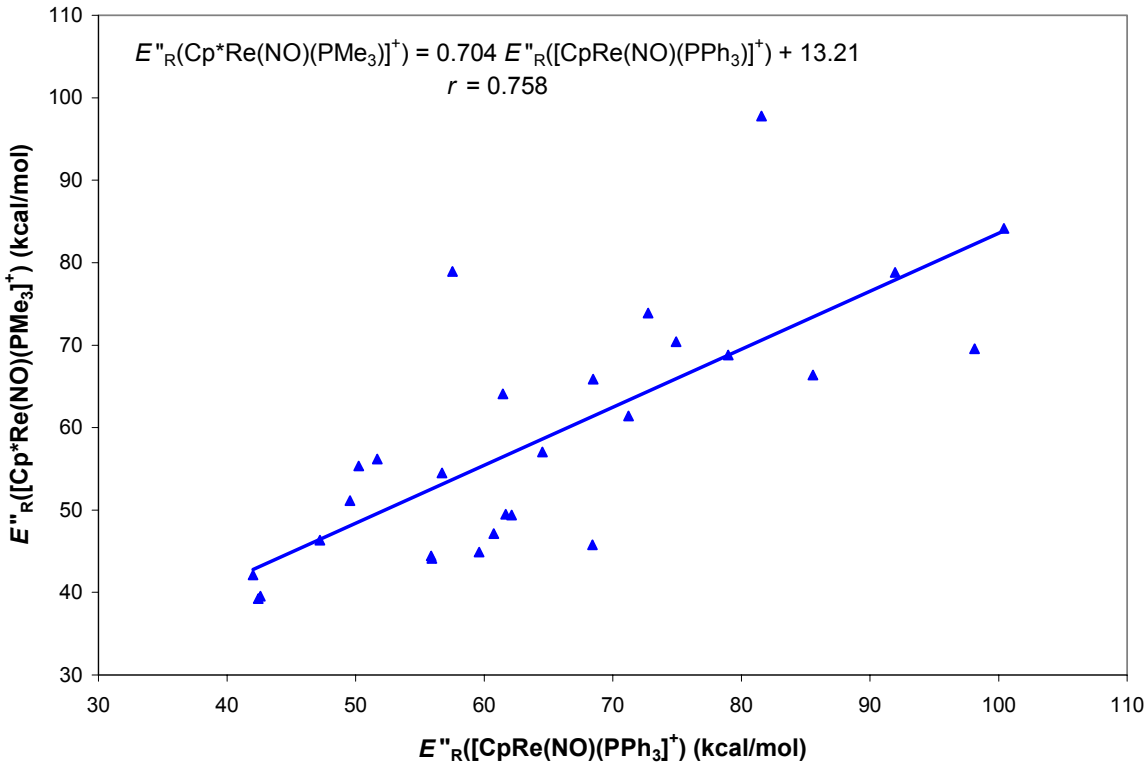

Figure 5. Plot of ligand repulsive energy computed for the olefins listed in Table 3 computed with the $[Cp^*Re(NO)(PMe_3)]^+$ fragment versus the ligand repulsive energies computed with the $[CpRe(NO)(PPh_3)]^+$ fragment.

3.3 Computational Estimate of Diastereoselectivity Using PM3(tm) Energies

There are two factors that determine whether a conformer can effectively participate in a chemical reaction: low internal energy (high Boltzmann population) and low ligand repulsive energy (efficient olefin binding). In order to determine the Boltzmann weight of isomer i, w_i, the PM3(tm) heat of formation for isomer i, ΔH_i, relative to the heat of formation of the lowest energy isomer, ΔH_0 are needed. Then, the Boltzmann weight is given by

$$w_i = \frac{\exp\left(-\dfrac{\Delta H_i - \Delta H_0}{kT}\right)}{\sum_i \exp\left(-\dfrac{\Delta H_i - \Delta H_0}{kT}\right)} \tag{2}$$

where k is the Boltzmann constant and T is the temperature in Kelvin. At 298.15 K, kT = 0.592476141388 kcal/mol. If we assume that diastereoselective excess, *de*, is determined only by the energy of the isomer and not influenced by the ligand repulsive energy, then there should be a correlation between computed and experimentally determined *de*. Using PM3(tm) energy alone, we define

$$de_{\mathrm{SEQM'}} = \left(w_{RS,SR} + w_{RS,SR2}\right) - \left(w_{RR,SS} + w_{RR,SS2}\right) \tag{3}$$

where $w_{RS,SR}$ is the Boltzmann weight of the energy of the *RS,SR* isomer, as defined in Figure 1, $w_{RS,SR2}$ is the Boltzmann weight of the energy of the *RS,SR*2 isomer, etc. There is no correlation between $de_{\mathrm{SEQM'}}$ and experimental *de* values measured by Gladysz for the $[\mathrm{CpRe(NO)(PPh_3)}]^+$ fragment ($r = 6 \times 10^{-3}$) [6]. Therefore, we conclude that the ligand repulsive energy of the olefin cannot be ignored in computing *de*.

An expression analogous to equation 2 can be defined for ligand repulsive energy alone. Diastereoselective excess determined using ligand repulsive energy, without taking into account ΔH for the isomer, also correlates poorly with experimental *de*, and has a negative slope. Therefore, we need a computational measure of diastereoselective excess that contains both ΔH and E''_{R} for the isomer.

We define a Boltzmann energy–weighted ligand repulsive energy for isomer i, $\langle E''_{\mathrm{R}}\rangle_i$, as

$$\left\langle E''_{\mathrm{R}}\right\rangle_i = w_i \times \frac{\exp\left(-\dfrac{\Delta E''_{\mathrm{R}}}{kT}\right)}{\sum_i \exp\left(-\dfrac{\Delta E''_{\mathrm{R}}}{kT}\right)} \tag{4}$$

We also define the SEQM–based diastereoselective excess, de_{SEQM}, as

$$de_{\mathrm{SEQM}} = \left(\left\langle E''_R\right\rangle_{RS,SR} + \left\langle E''_R\right\rangle_{RS,SR2}\right) - \left(\left\langle E''_R\right\rangle_{RR,SS} + \left\langle E''_R\right\rangle_{RR,SS2}\right) \tag{5}$$

where $\langle E''_{\mathrm{R}}\rangle_{RS,SR}$ is the Boltzmann weighted E''_{R} value for the *RS,SR* isomer as defined in Table 1, etc. Both w_i and $\langle E''_{\mathrm{R}}\rangle_i$ values are listed in Tables 3 and 4. The correlation between experimental *de* and de_{SEQM} is poor ($r = 0.008$); SEQM heats of formation may not be accurate enough to weight the E''_{R} values in order to obtain a good correlation between computed and experimental *de*. Therefore, we have undertaken a DFT approach to the problem, which is in progress in our laboratories.

Even though there is no quantitative relationship between experimental and computed *de*, we can use the de_{SEQM} values to rank the efficacy of a complex towards stereoselective binding of a prochiral α–olefin. When we plot total fragment cone angle versus de_{SEQM}, we obtain an excellent linear relationship (Figure 6).

As the steric congestion in the fragment increases, so de_{SEQM} increases linearly. This means that the greater the congestion, the greater the repulsion experienced by an incoming olefin. This

argument reinforces the hypothesis presented by Gladysz in order to rationalize the trends in experimental *de* [6].

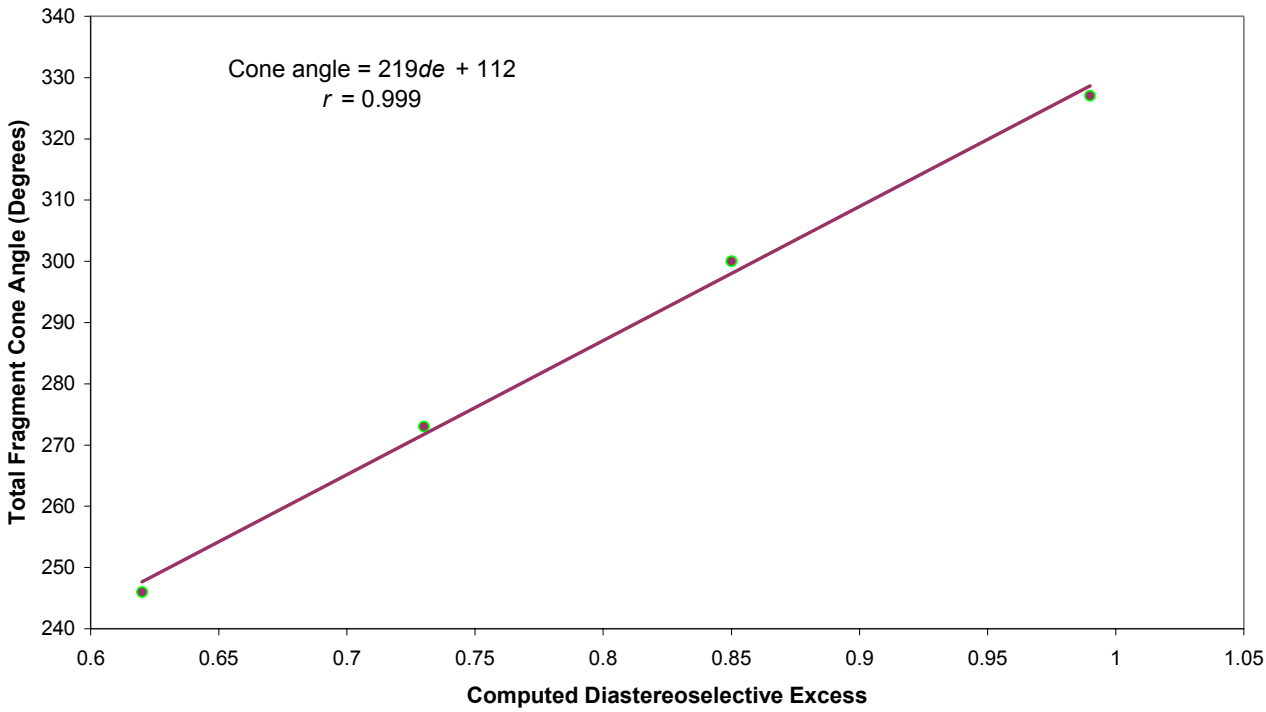

Figure 6. Plot of total fragment cone angle (cone angle for cyclopentadienyl ligand plus NO plus phosphine) versus computed diastereoselective excess defined in equation (5).

The nonzero intercept in the plot of total fragment cone angle versus de_{SEQM} indicates the presence of a steric threshold. In other words, no diastereoselectivity is observed unless the total fragment cone angle exceeds 112º. Since the cone angle of the cyclopentadienyl ligand is 128º [7,16,29], it is difficult to design an organorhenium fragment that falls below this steric threshold.

4 CONCLUSIONS

Using PM3(tm), geometry optimized structures for $[(\eta^5\text{–}C_5R_5)Re(\eta^2\text{–}CH_2{=}CHR')(NO)(L)]^+$ (R = H, Me; R′ = Me, *n*–Pr, Bn, Ph, *i*–Pr, *t*–Bu, $SiMe_3$; L = PMe_3, PPh_3) complexes have been generated, which closely match structural parameters reported in the CSD [21]. A genetic algorithm optimized PM3(tm) Hamiltonian was used to obtain heats of formation for the $[(\eta^5\text{–}C_5R_5)Re(\eta^2\text{–}CH_2{=}CHR')(NO)(L)]^+$ complexes. Brown's MM–based ligand repulsive energy parameter was used to compute steric size of the olefins in the $[(\eta^5\text{–}C_5R_5)Re(NO)(L)]^+$ environments. Ligand repulsive energies allowed the sizes of the four fragments to be ranked in terms of steric demand from the perspective of the α–olefins. A Boltzmann–averaged diastereoselective excess was defined and found to increase as the steric bulk of the $[(\eta^5\text{–}C_5R_5)Re(NO)(L)]^+$ fragment increases. A steric threshold was discovered at a total fragment cone angle of 112º. Therefore, in order to optimize

diastereoselective binding of a prochiral olefin by a chiral organorhenium fragment, steric congestion of the order of that in $[Cp^*Re(NO)(PPh_3)]^+$ needs to be built into the chiral Lewis acid.

Acknowledgment

We thank the NSF through grant CHE–0111131 for funding.

5 REFERENCES

[1] L. S. Hegedus, *Transition Metals in the Synthesis of Complex Organic Molecules*, 2nd ed., University Science Books, Sausalito, CA, 1999.
[2] J. S. Giovannetti, C. M. Kelly, and C. R. Landis, Molecular Mechanics and NOE Investigations of the Solution Structures of Intermediates in the [Rhodium(Chiral Bisphosphine)]$^+$–Catalyzed Hydrogenation of Prochiral Enamides, *J. Am. Chem. Soc.* **1993**, *115*, 4040–4057.
[3] C. R. Landis, P. Hilfenhaus, and S. Feldgus, Structures and Reaction Pathways in Rhodium(I)–Catalyzed Hydrogenation of Enamides: A Model DFT Study, *J. Am. Chem. Soc.* **1999**, *121*, 8741–8754.
[4] C. R. Landis and S. Feldgus, A Simple Model for the Origin of Enantioselection and the "Anti–Lock–and–Key" Motif in Asymmetric Hydrogenation of Enamide as Catalyzed by Chiral Diphosphine Complexes of Rh(I), *Organometallics* **2001**, *20*, 2374–2387.
[5] A. M. Gillespie and D. P. White, Understanding the Steric Control of Stereoselective Olefin Binding in Cyclopentadienyl Complexes of Rhenium: An Application of *De Novo* Ligand Design, *Organometallics* **2001**, *20*, 5149–5155.
[6] J. A. Gladysz and B. J. Boone, Chiral Recognition in Π Complexes of Alkenes, Aldehydes, and Ketones with Transition Metal Lewis Acids; Development of a General Model for Enantioface Binding Selectivities, *Angew. Chem. Int. Ed. Engl.* **1997**, *36*, 550–583.
[7] D. White and N. J. Coville, Quantification of Steric Effects in Organometallic Chemistry, *Adv. Organomet. Chem* **1994**, *36*, 95–158.
[8] T. L. Brown, A Molecular Mechanics Model of Ligand Effects. 3. A New Measure of Ligand Steric Effects, *Inorg. Chem.* **1992**, *31*, 1286–1294.
[9] M.–G. Choi and T. L. Brown, A Molecular Mechanics Model of Ligand Effects. 4. Binding of Amines to $Cr(Co)_5$: E_R Values for Amines, *Inorg. Chem.* **1993**, *32*, 1548–1553.
[10] M.–G. Choi and T. L. Brown, A Molecular Mechanics Model of Ligand Effects. 5. Ligand Repulsive Energy Values for Phosphines and Phosphites Bound to CpRhCO and the Crystal Structure of $CpRh(CO)(PPh_3)$, *Inorg. Chem.* **1993**, *32*, 5603–5610.
[11] M.–G. Choi, D. White, and T. L. Brown, A Molecular Mechanics Model of Ligand Effects. 6. Binding of Group 16 Donor Ligands to $Cr(Co)_5$: E_R Values for Alcohols, Ethers, and Thioethers, *Inorg. Chem.* **1994**, *33*, 5591–5594.
[12] D. P. White and T. L. Brown, Molecular Mechanics Model of Ligand Effects 7. Binding of η^2 Ligands to $Cr(CO)_5$ and CpRh(CO): E_R Values for Olefins, *Inorg. Chem.* **1995**, *34*, 2718–2724.
[13] D. P. White, J. C. Anthony, and A. O. Oyefeso, Computational Measurement of Steric Effects: The Size of Organic Substituents Computed by Ligand Repulsive Energies, *J. Org. Chem.* **1999**, *64*, 7707–7716.
[14] R. J. Bubel, W. Douglass, and D. P. White, Molecular Mechanics–Based Measures of Steric Effects: Customized Code to Compute Ligand Repulsive Energies, *J. Comput. Chem.* **2000**, *21*, 239–246.
[15] D. P. White, in: *Computational Organometallic Chemistry*; Ed. T. R. Cundari, Marcel–Dekker, New York, 2001, pp. 39 – 69.
[16] T. L. Brown and K. J. Lee, Ligand Steric Properties, *Coord. Chem. Rev.* **1993**, *128*, 89–116.
[17] *Cerius^2 4.5*, Accelrys, San Diego, CA, 2001.
[18] A. K. Rappé, C. J. Casewit, K. S. Colwell, W. A. Goddard, III, and W. M. Skiff, UFF, a Full Periodic Table Force Field for Molecular Mechanics and Molecular Dynamics Simulations, *J. Am. Chem. Soc.* **1992**, *114*, 10024–10035.
[19] Spartan version 5.1.3, Wavefunction, 18401 Von Karman Avenue, Suite 370, Irvine, CA 92612.
[20] T. R. Cundari, J. Deng, and W. Fu, Genetic Algorithm Optimization of Semiempirical Parameters for Transition Metals, *Intern. J. Quantum Chem.* **2000**, *77*, 421–432.
[21] F. H. Allen and O. Kennard, Cambridge Structural Data Center October 2001 Release, *Chem. Design Autom. News* **1993**, *8*, 31–37.
[22] B. E. R. Schilling, R. Hoffmann, and J. W. Faller, Effect of Ligand Asymmetry on the Structure and Reactivity of CpMLL'(Allyl) and –(Ethylene) Complexes, *J. Am. Chem. Soc.* **1979**, *101*, 592–598.

[23] W. A. Kiel, G.–Y. Lin, A. G. Constable, F. B. McCormick, C. E. Strouse, O. Eisenstein, and J. A. Gladysz, Synthesis and Properties of $[(\eta–C_5H_5)Re(NO)(PPh_3)(=CHC_6H_5)]^+PF_6^-$: A Benzylidene Complex That Is Formed by a Stereospecific α–Hydride Abstraction, Exists as Two Geometric Isomers, and Undergoes Stereospecific Nucleophilic Attack, *J. Am. Chem. Soc.* **1982**, *104*, 4865.
[24] P. T. Czech, J. A. Gladysz, and R. F. Fenske, The Role of Virtual Halogen D Orbitals in the Stability and Reactivity of Rhenium Alkyl Halide Complexes of The Form $[(\eta^5–C_5H_5)Re(NO)(PPh_3)(XR)]^+$, *Organometallics* **1989**, *8*, 1810.
[25] A. K. Rappé, K. S. Colwell, and C. J. Casewit, Application of a Universal Force Field to Metal Complexes, *Inorg. Chem.* **1993**, *32*, 3438–3450.
[26] N. L. Allinger, Conformational Analysis. 130. MM2. A Hydrocarbon Force Field Utilizing V1 and V2 Torsional Terms, *J. Am. Chem. Soc.* **1977**, *99*, 8127–8134.
[27] J. T. Sprague, J. C. Tai, Y. Yuh, and N. L. Allinger, The MMP2 Calculational Method, *J. Comput. Chem.* **1987**, *8*, 581–603.
[28] C. A. Tolman, *J. Am. Chem. Soc.* **1970**, *92*, 2953.
[29] C. A. Tolman, Steric Effects of Phosphorus Ligands in Organometallic Chemistry and Homogeneous Catalysis, *Chem. Revs.* **1977**, *77*, 313–348.

Biographies

David P. White, Ph.D., is assistant professor of chemistry at the University of North Carolina at Wilmington. Dr. White formulated the Wilmington Investigation into the Structural Design of Organometallic Materials (WISDOM) in 1999. After obtaining a Ph.D. degree in synthesis and mathematical modeling of organometallic complexes from the University of the Witwatersrand in Johannesburg, Dr. White undertook postdoctoral research with Professor Theodore L. Brown at the Beckman Institute for Advanced Science and Technology at the University of Illinois at Urbana–Champaign. More recently, Dr. White has collaborated on projects with Professor Thomas R. Cundari of Computational Research on Materials Institute at the University of Memphis (CROMIUM).

Aaron M. Gillespie is an undergraduate research student working on computational chemistry in WISDOM at the University of North Carolina at Wilmington. Mr. Gillespie has also worked on computational chemistry projects at the Computational Research on Materials Institute at the University of Memphis (CROMIUM) with Drs. David White and Thomas R. Cundari.